Electronic Supplementary Material (ESI) for Nanoscale.
This journal is © The Royal Society of Chemistry 2024

**Supporting Information for**

# Bridging Colloidal and Electrochemical Syntheses of Metal Nanocrystals with Seeded Electrodeposition for Tracking Single Nanocrystal Growth

*Ekta Verma,[a] Myung-Hoon Choi,[b,c] Nabojit Kar,[a] Lane A. Baker,[b] and Sara E. Skrabalak*[*a]*

[a]Department of Chemistry, Indiana University–Bloomington, Bloomington, Indiana, 47405, USA

[b]Department of Chemistry, Texas A & M University, College Station, Texas, 77843, USA

[c]Current Affiliation: Research Application Center, Park Systems Inc., Santa Clara, California, 95054, USA

*sskrabal@indiana.edu

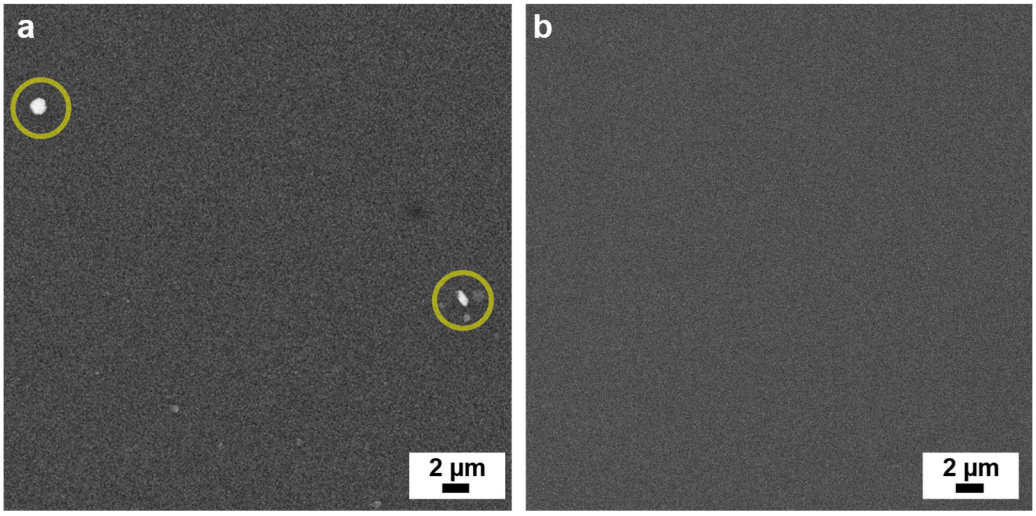


**Figure S1.** (a) SEM images of GCEs after polishing with alumina slurry in the order of 1.0, 0.5, and 0.05 µm particle diameters and (b) after additional polishing using a wet polishing pad.

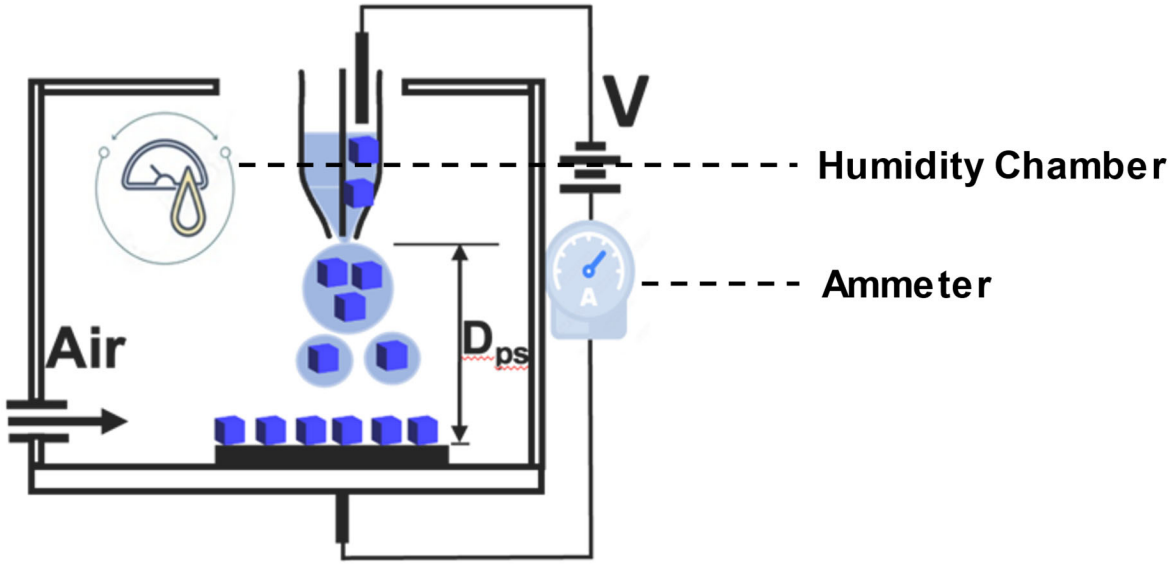


**Figure S2**. Diagram for electrospray (ES) deposition setup showing a pipette positioned at a spray distance (Dps). Air flow maintains a low relative humidity and an ammeter reads the ES current for ES deposition.

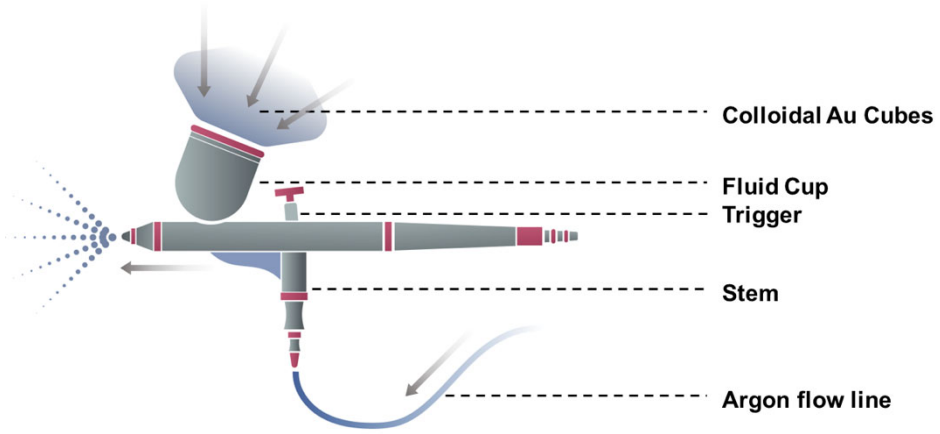


**Figure S3.** Schematic of the airbrush showing a fluid cup filled with colloidal Au nanocube solution and the stem connected to an argon (Ar) tank for the air flow.

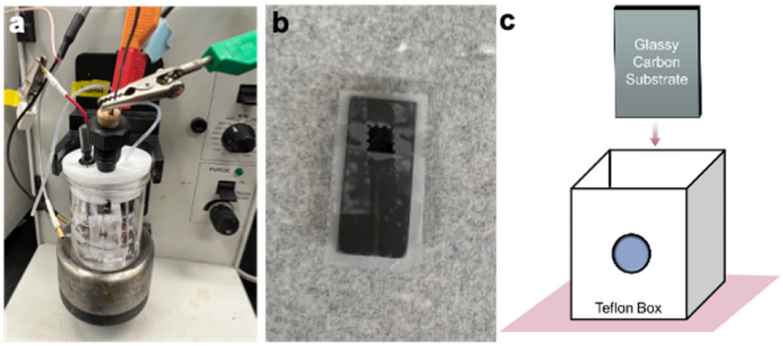


**Figure S4.** Photograph of (a) the three-electrode electrochemistry setup and (b) GCE with tape mask. (c) Schematic of the Teflon box and the GCE.

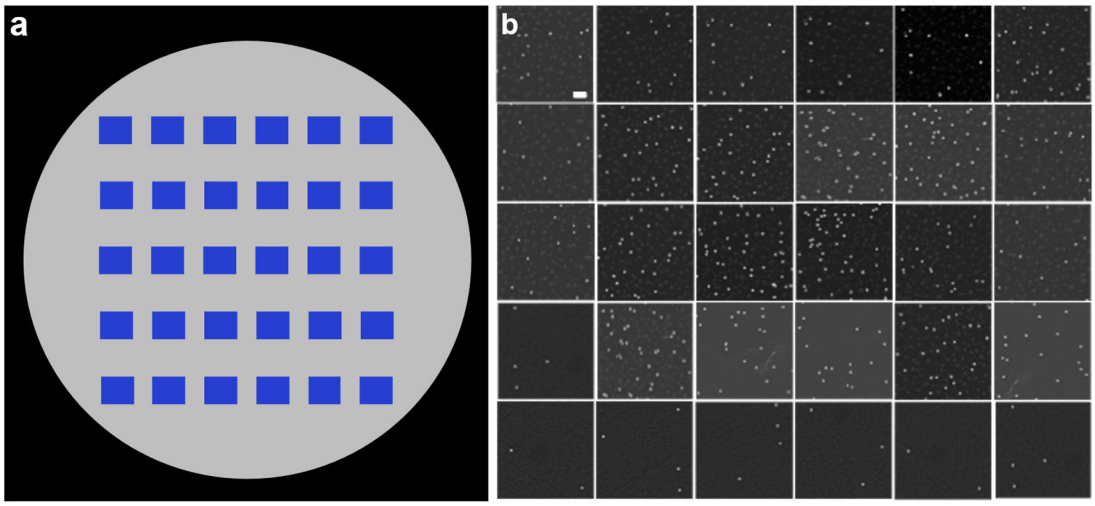


**Figure S5.** (a) Schematic showing the positions within the ES deposition spot that were imaged by SEM. (b) SEM images from regions denoted in (a). Scale bar 400 nm applied to all SEM frames.

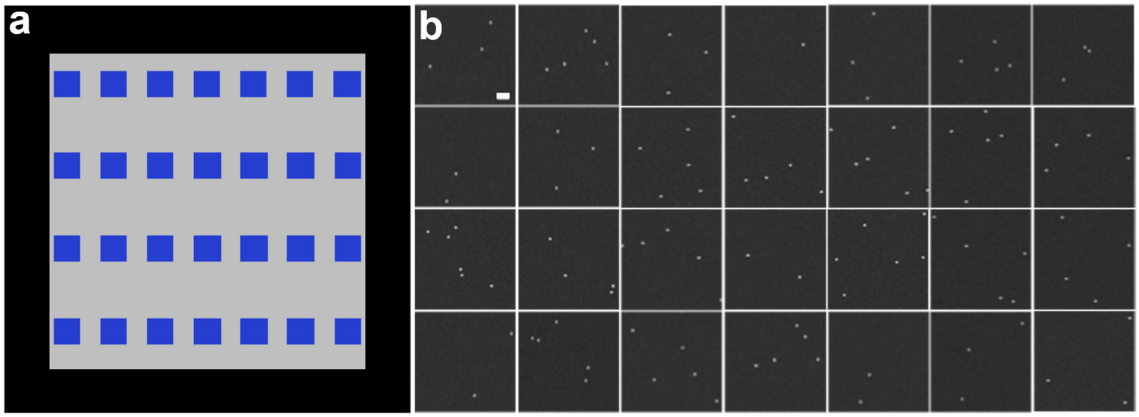


**Figure S6.** (a) Schematic showing the positions within the airbrushed region that were analyzed by SEM. (b) SEM images from regions denoted in (a). Scale bar 400 nm applies to all SEM frames.

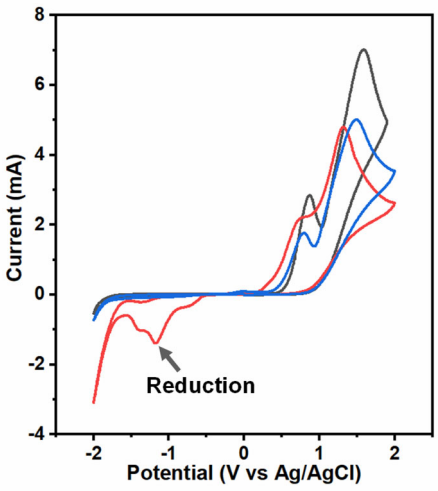


**Figure S7.** Cyclic voltammograms of a GCE in only 0.32 M $Na_2SO_3$ electrolyte solution (blue line), 2 µL 0.346 mM Au nanocubes concentration dropcast on GCE in 0.32 M $Na_2SO_3$ electrolyte solution (black line), and 2 µL 0.346 mM Au nanocubes concentration dropcast on GCE in 0.32 M $Na_2SO_3$ electrolyte solution, and 6.3 µM $Na_3Au(SO_3)_2$ (red line).

*Discussion of Cyclic Voltammetry of Au Precursor*

In traditional colloidal syntheses, the most common Au precursor is $HAuCl_4$; however, for electrochemical syntheses of Au NCs,[1,2,3,4,5,6] a Au(I) salt is preferred because only one electron is required to reduce it making the interpretation of the results more straightforward when coupled with constant potential methods. Common Au (I) salts include gold cyanide,[7,] gold sulfite[9] and gold thiosulfate,[10] which have been reported in electrodeposition.[11] Gold cyanide is an attractive precursor as it is resistant to disproportionation, hydrolysis, oxidation, and decomposition, but gold cyanide is highly toxic.[12] In contrast, sodium gold sulfite is non-toxic, and handling and disposal is easier than other gold precursors.[13] Also, it can produce thick gold electrodeposits that are smooth and bright, suggesting it would be suitable in seeded electrodeposition.[14,15] The stability constant of sodium gold sulfite is high and can operate at basic conditions with pH>9. Thus, sodium gold sulfite as a gold precursor was used here in seeded electrodeposition.

Cyclic voltammetry (CV) was used to investigate the behavior of redox-active species in solution and informed the design the electrodeposition experiments. The scan started at 0 V going in the negative direction and then moved backwards. Figure S7 shows the voltametric behavior of the sodium sulfite ($Na_2SO_3$) electrolyte (blue line) and Au nanocubes on GCE in $Na_2SO_3$ electrolyte (black line); both curves show no cathodic peak but have an oxidation peak in the reverse scan. Further, the voltametric behavior of Au nanocubes on GCE in 6.3 μM sodium gold (I) sulfite with 0.32 M $Na_2SO_3$ electrolyte (pH= 9.63) is shown in red line. When scanning in the negative direction, the rising cathodic current at -1.175 V *vs.* Ag/AgCl indicates reduction of the Au precursor. In the reverse scan, no characteristic peak for the oxidation of Au precursor was observed. All CVs were collected at a scan rate of 100 mV/s. For initial electrodeposition experiments, the reduction potential of the Au precursor was chosen (*i.e.,* -1.175 V *vs.* Ag/AgCl).

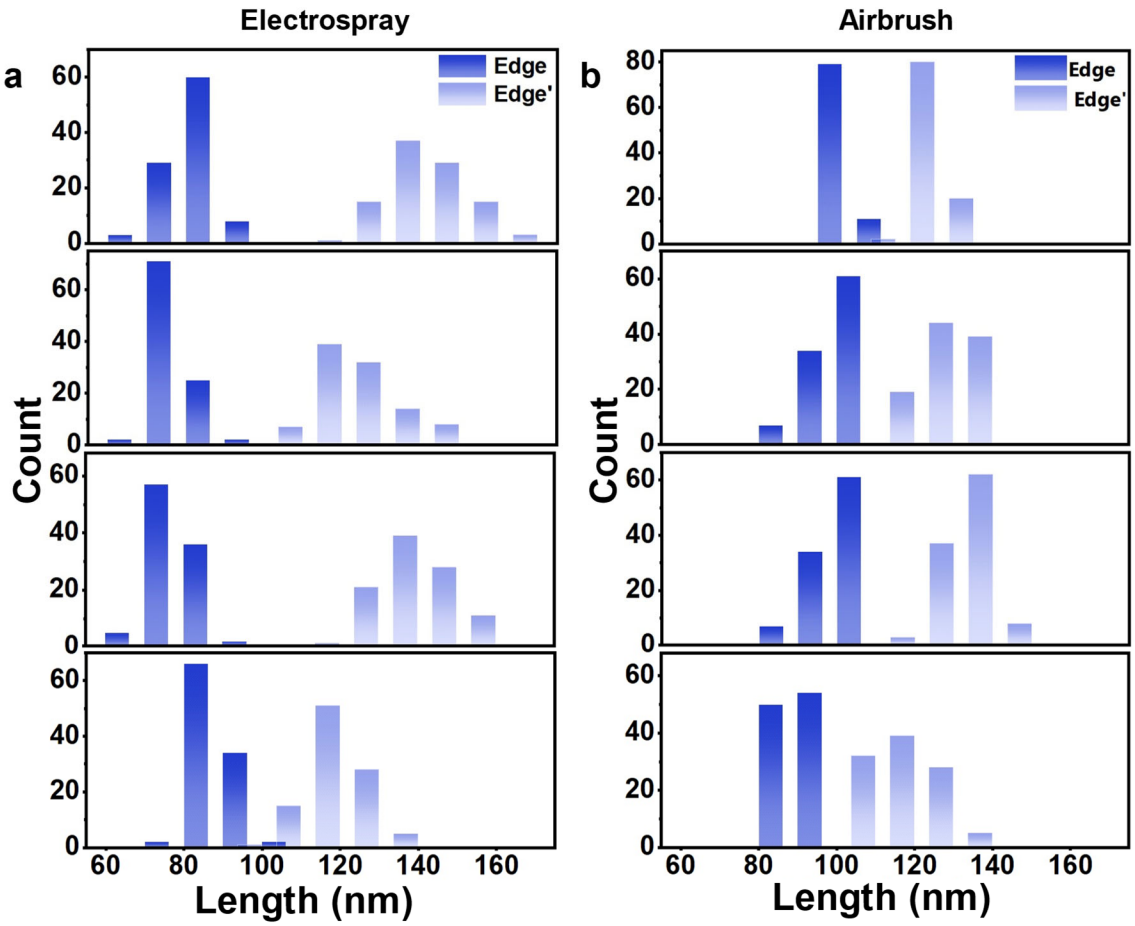


**Figure S8.** Size histograms from four Au electrodeposition experiments where Au nanocubes were deposited by (a) electrospray and (b) airbrush using the same conditions (applied potential of -1.175 V *vs.* Ag/AgCl for 10 min in 3.5 μM $Na_3Au(SO_3)_2$ and 0.32 M $Na_2SO_3$ electrolyte solution). Distribution of measured edge lengths of the Au nanocubes before Au electrodeposition is shown in dark blue (Edge) and after electrodeposition in light blue (Edge′).

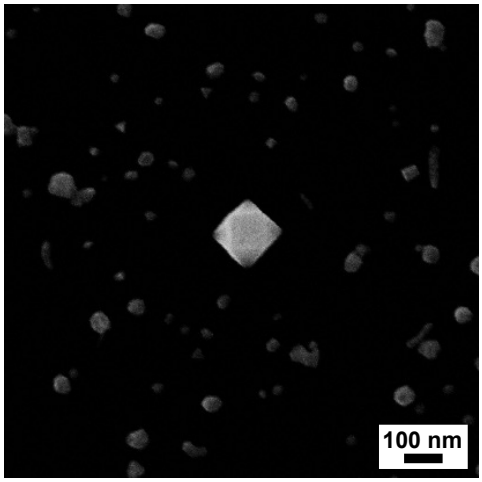


**Figure S9**. SEM image of product after constant potential electrolysis for 10 min at -1.175 V *vs.* Ag/AgCl at lower concentration of $Na_3Au(SO_3)_2$ (0.35 μM) compared to higher concentration of $Na_3Au(SO_3)_2$ (3.5 $\mu$M, Fig.1) with Au nanocubes deposited on the GCE by airbrush.

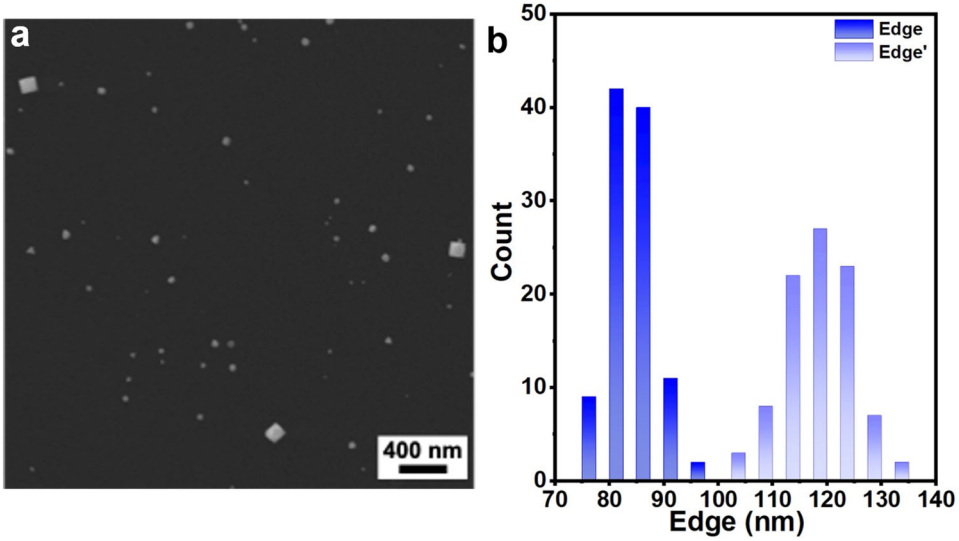


**Figure S10.** (a) Low magnification SEM image of electrodeposited product (-1.075 V *vs*. Ag/AgCl for 10 min at 0.35 μM $Na_3Au(SO_3)_2$ and 0.32 M $Na_2SO_3$ electrolyte. (b) Size histogram, where the distribution of measured edge lengths of the Au nanocubes before Au electrodeposition is shown in dark blue (Edge) and after electrodeposition in light blue (Edge′).

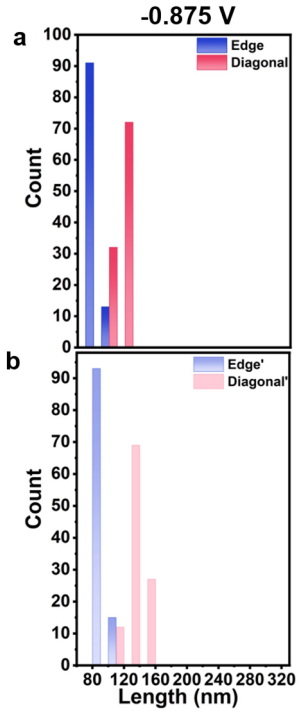


**Figure S11.** Size histogram shows the distribution of measured edge lengths and diagonal lengths of Au nanocubes (a) before electrodeposition (Edge/Diagonal in Blue/Pink) and (b) after electrodeposition (Edge′/Diagonal′ in light Blue/Pink) at -0.875 V *vs.* Ag/AgCl for 10 min in 0.35 μM $Na_3Au(SO_3)_2$ and 0.32 M $Na_2SO_3$ electrolyte.

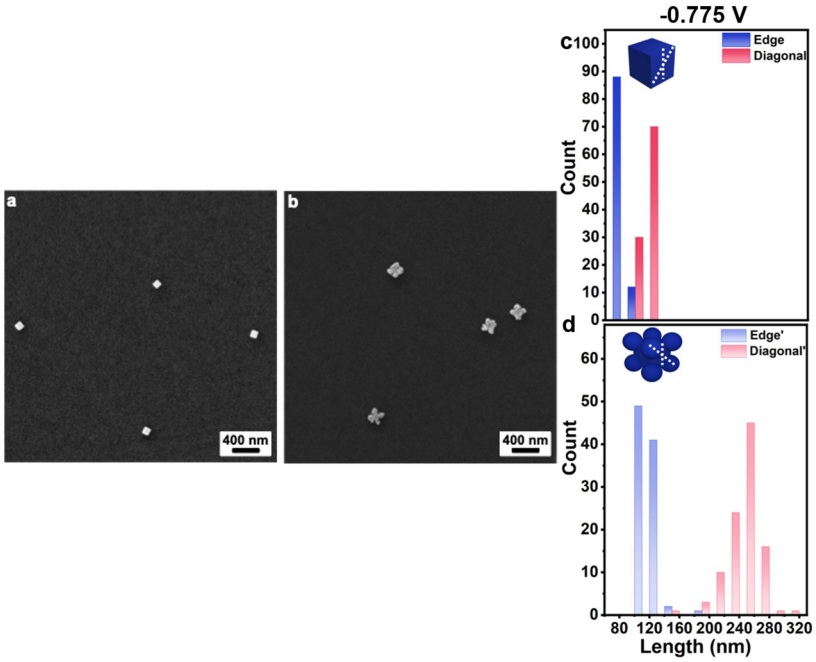


**Figure S12.** SEM images of (a) Au nanocubes before electrodeposition and (b) corner-deposited nanocrystal product obtained after electrodeposition at -0.775 V *vs.* Ag/AgCl for 10 min in 0.35 μM $Na_3Au(SO_3)_2$ and 0.32 M $Na_2SO_3$ electrolyte. (c) Size histogram showing the distribution of measured edge and diagonal lengths of the Au nanocubes before Au electrodeposition (Edge/Diagonal in Blue/Pink), and (d) after Au electrodeposition (Edge′/Diagonal′ in light Blue/Pink).

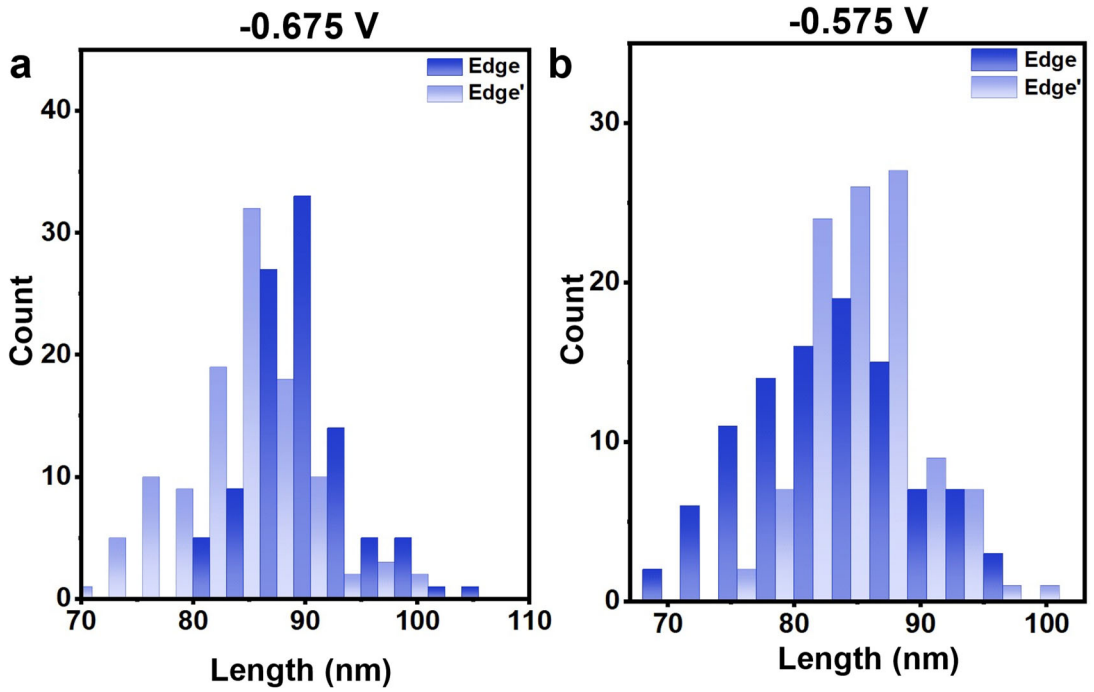


**Figure S13.** Size histograms showing the edge lengths of Au nanocubes (a) at -0.675 V *vs.* Ag/AgCl and (b) -0.575 V *vs.* Ag/AgCl for 10 min in 0.35 μM $Na_3Au(SO_3)_2$ and 0.32 M $Na_2SO_3$ electrolyte, where before electrodeposition is shown in dark blue (Edge) and after electrodeposition in light blue (Edge′).

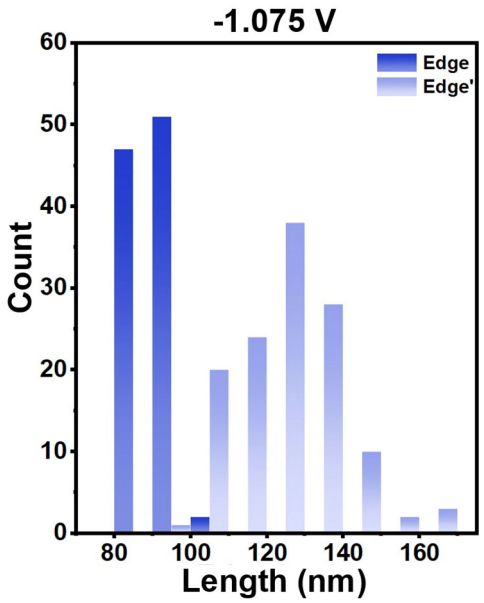


**Figure S14.** Size histogram analysis of edge lengths of Au nanocubes before electrodeposition is shown in dark blue (Edge) and of the product after electrodeposition in light blue (Edge′) at -1.075 V *vs.* Ag/AgCl for 15 min at 0.35 μM $Na_3Au(SO_3)_2$ and 0.32 M $Na_2SO_3$ electrolyte.

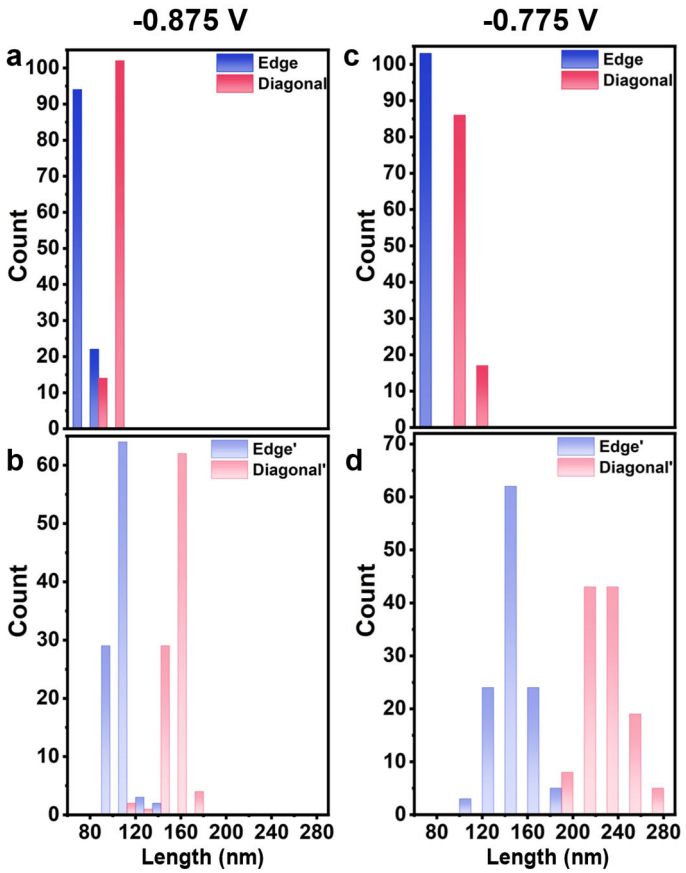


**Figure S15.** Size histogram analysis of edge and diagonal lengths of (a) Au nanocubes before electrodeposition (Edge/Diagonal in Blue/Pink), and of (b) the electrodeposited product (Edge′/Diagonal′ in light Blue/Pink) at -0.875 V *vs.* Ag/AgCl for 15 min. Size histogram analysis of (c) Au nanocubes before electrodeposition and of (d) the product after electrodeposition at -0.775 V *vs.* Ag/AgCl for 15 min. Both in 0.35 μM $Na_3Au(SO_3)_2$ and 0.32 M $Na_2SO_3$ electrolyte.

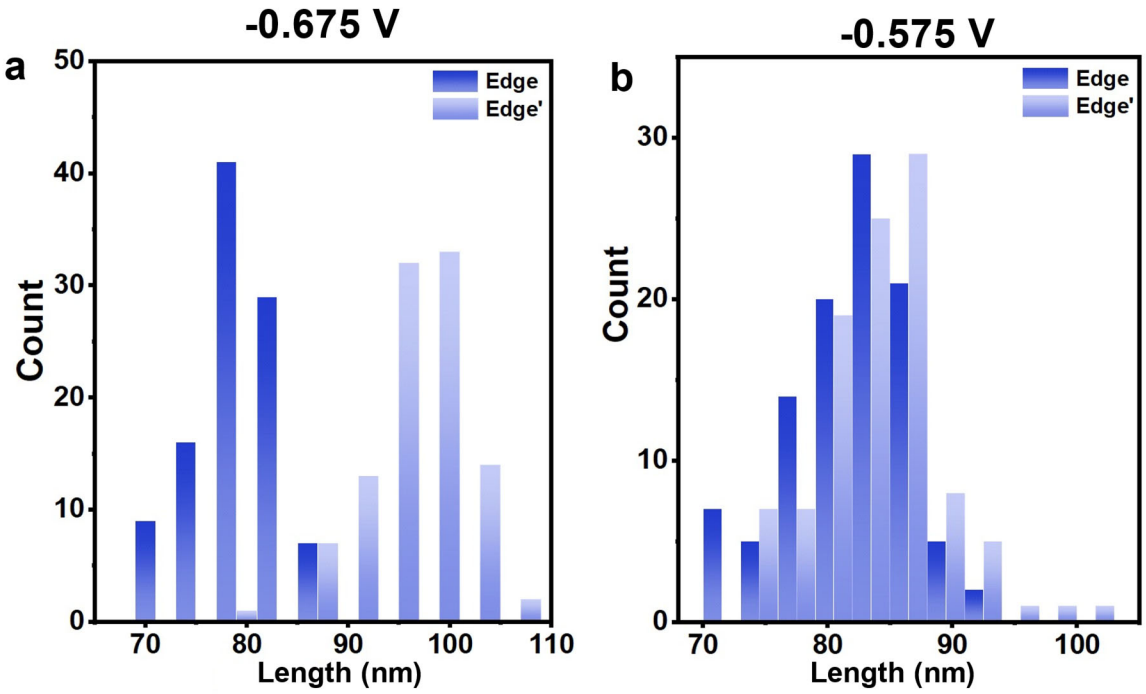


**Figure S16**. Size histogram analysis of edge lengths of Au nanocubes before electrodeposition is shown in dark blue (Edge) and of the product after electrodeposition (Edge′) in light blue. (a) at -0.675 V *vs.* Ag/AgCl for 15 min and (b) -0.575 V *vs.* Ag/AgCl for 15 min. Both in 0.35 μM $Na_3Au(SO_3)_2$ and 0.32 M $Na_2SO_3$ electrolyte.

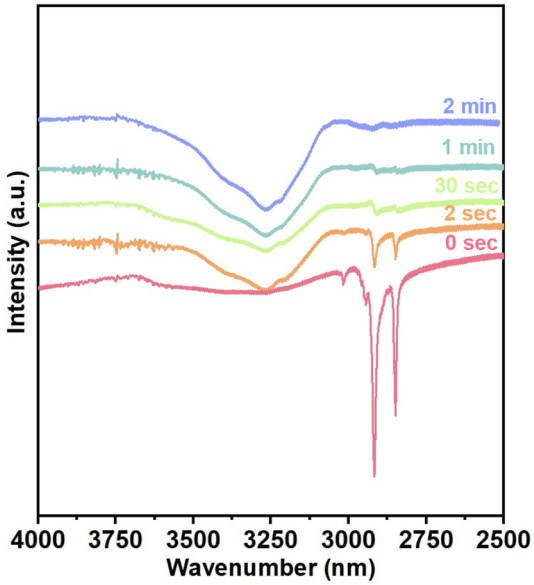


**Figure S17.** FTIR spectra of Au nanocubes was taken by drpocasting the Au nanocubes on glass slide then dried to adhere the Au nanocubes to the slide. The slide was then soaked in methanol for different periods of time: 0 sec (pink), 2 sec (orange), 30 sec (green), 1 min (cyan) and 2 min (blue). The slide was then dried and the FTIR spectrum obtained.

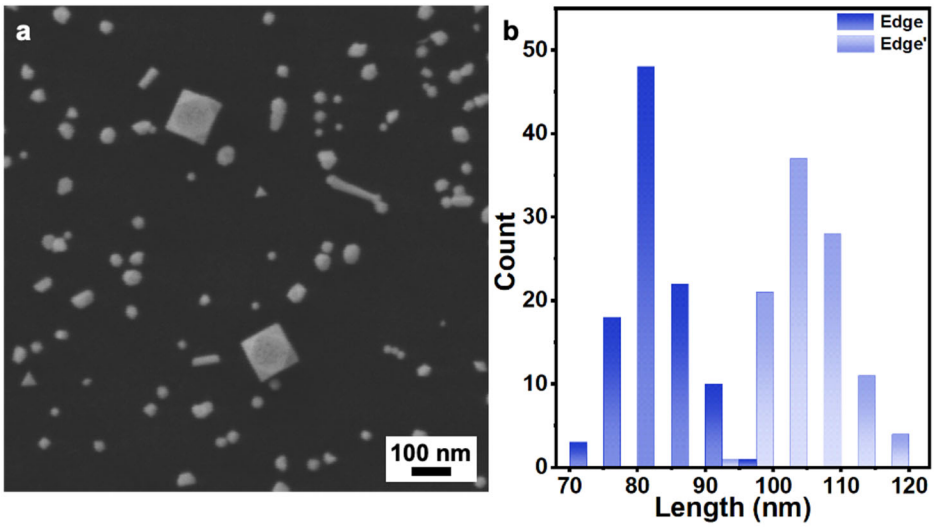


**Figure S18.** (a) SEM image of electrodeposited product (-1.175 V *vs.* Ag/AgCl for 10 min after CTAB removal in 3.5 μM $Na_3Au(SO_3)_2$ and 0.32 M $Na_2SO_3$ electrolyte). (b) Size histogram, where the distribution of measured edge lengths of the Au nanocubes before Au electrodeposition is shown in dark blue and after electrodeposition in light blue.

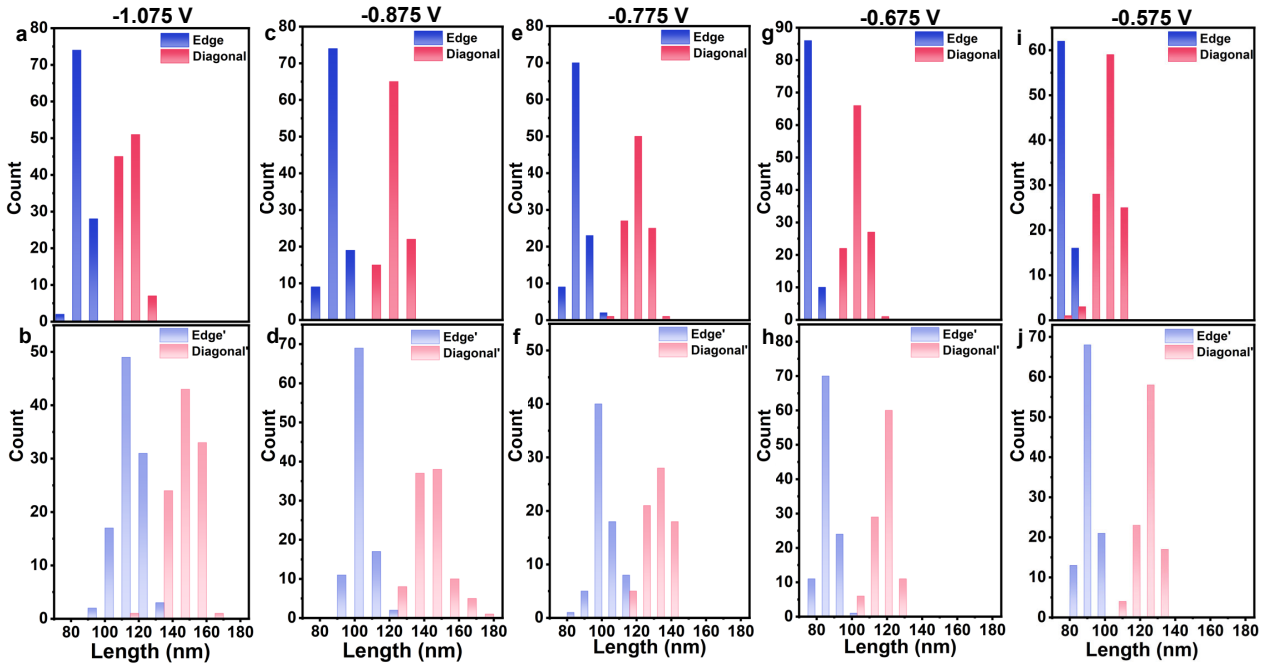


**Figure S19.** Size histogram showing (a,c,e,g,i) edge and diagonal lengths of the Au nanocubes before electrodeposition (Edge/Diagonal in Blue/Pink) and (b,d,f,h,j) of the electrodeposited-product obtained after electrodeposition (Edge′/Diagonal′ in light Blue/Pink) at -1.075 V *vs.* Ag/AgCl, -0.875 V *vs.* Ag/AgCl, -0.775 V *vs.* Ag/AgCl, -0.675 V *vs.* Ag/AgCl, and -0.575 V *vs.* Ag/AgCl respectively for 10 min after CTAB removal in 0.35 µM $Na_3Au(SO_3)_2$ and 0.32 M $Na_2SO_3$ electrolyte.

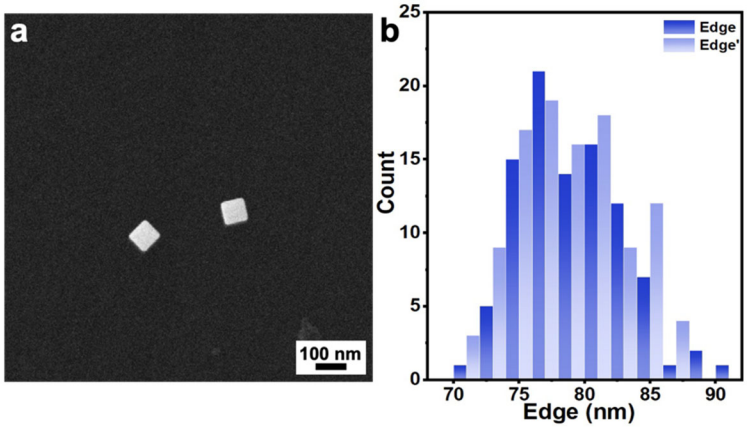


**Figure S20.** (a) SEM image of electrodeposited product (-0.475 V *vs.* Ag/AgCl for 10 min after CTAB removal in 0.35 μM $Na_3Au(SO_3)_2$ and 0.32 M $Na_2SO_3$ electrolyte). (b) size histogram, where the distribution of measured edge lengths of the Au nanocubes before Au electrodeposition is shown in dark blue and after electrodeposition in light blue.

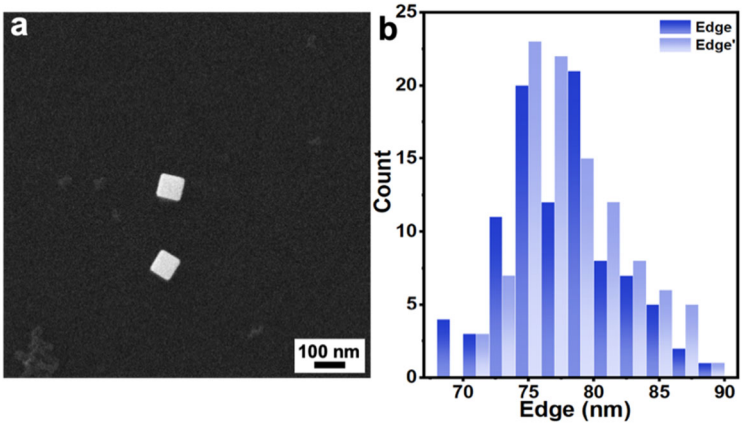


**Figure S21.** (a) SEM image of electrodeposited product (-0.375 V *vs.* Ag/AgCl for 10 min after CTAB removal in 0.35 μM $Na_3Au(SO_3)_2$ and 0.32 M $Na_2SO_3$ electrolyte). (b) size histogram, where the distribution of measured edge lengths of the Au nanocubes before Au electrodeposition is shown in dark blue and after electrodeposition in light blue.

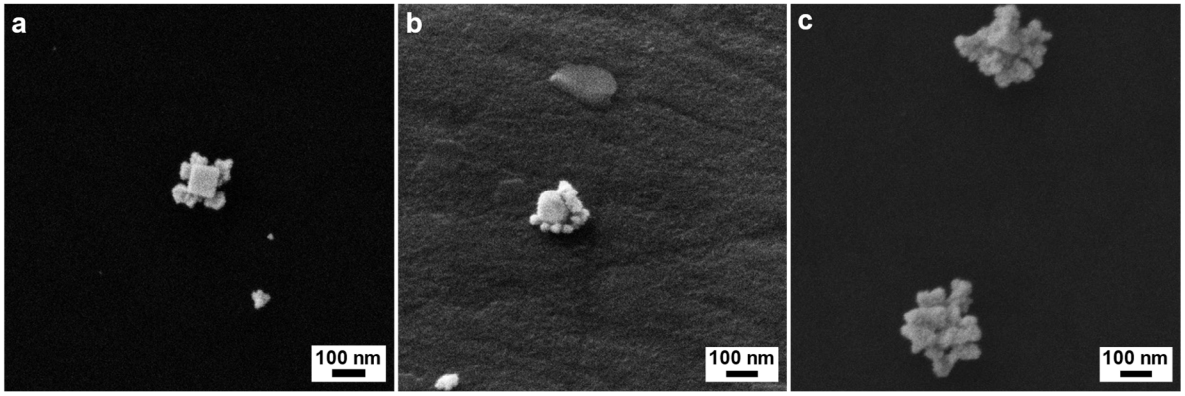


**Figure S22.** SEM images of electrodeposited product obtained after improper CTAB cleaning at -0.775 V *vs.* Ag/AgCl for 10 min in 0.35 μM $Na_3Au(SO_3)_2$ and 0.32 M $Na_2SO_3$ electrolyte.

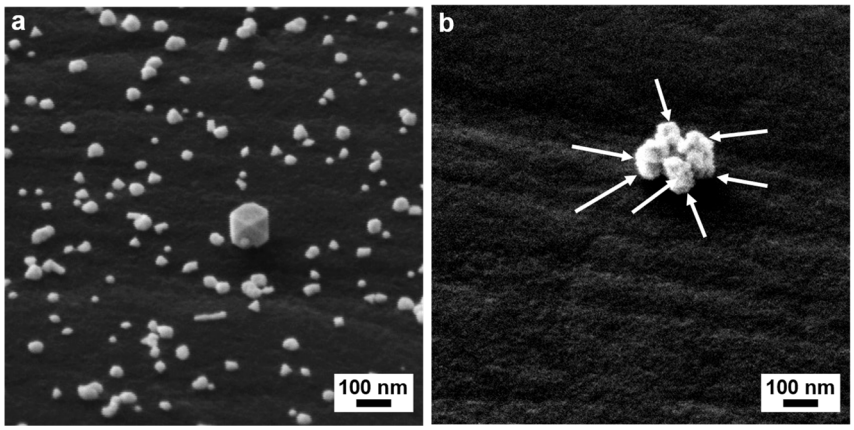


**Figure S23**. SEM images of electrodeposited product obtained at (a) -1.175 V *vs.* Ag/AgCl for 10 min and (b) -0.775 V *vs.* Ag/AgCl for 10 min. Both in 0.35 μM $Na_3Au(SO_3)_2$ and 0.32 M $Na_2SO_3$ electrolyte. The GCE was tilted by 54 degrees from right to left. The arrows in (b) are added to guide the reader's attention to seven regions of deposition.

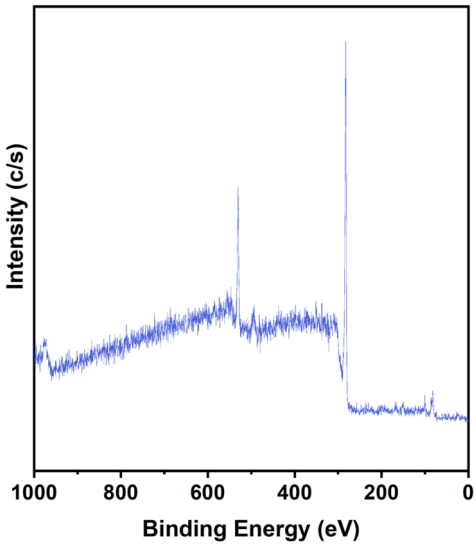


**Figure S24.** XPS survey spectrum of corner-deposited Au nanocubes obtained for electrodeposited product at -0.775 V *vs.* Ag/AgCl for 10 min in 3.5 μM $Na_3Au(SO_3)_2$ and 0.32 M $Na_2SO_3$ electrolyte indicating the observed element.

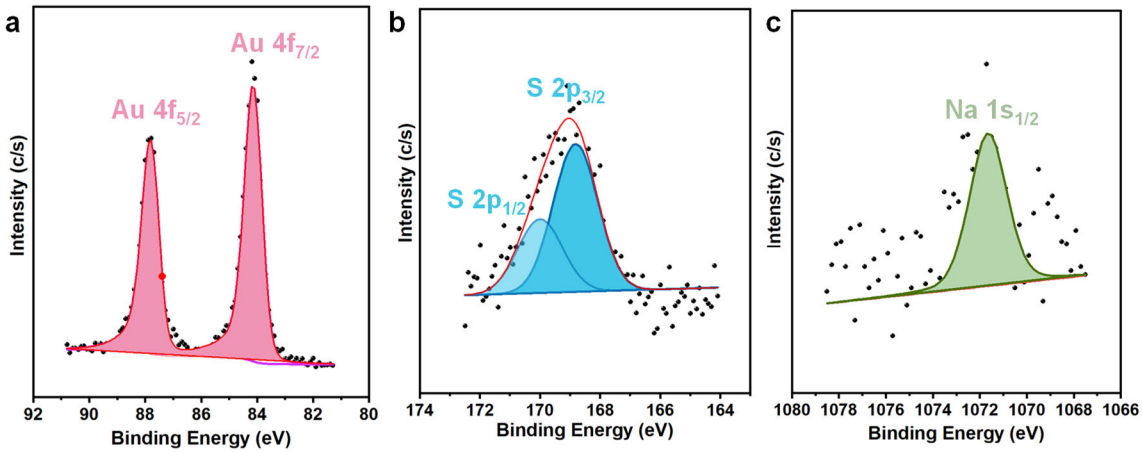


**Figure S25.** High resolution XPS spectra of the (a) Au 4f, (b) S 2p (c) Na 1s spectral regions for Au corner-deposited product obtained at -0.775 V *vs.* Ag/AgCl for 10 min in 3.5 μM $Na_3Au(SO_3)_2$ and 0.32 M $Na_2SO_3$ electrolyte. XPS analysis confirms the oxidation states of 0, 4+, and 1+ for Au, S and Na respectively.

The high-resolution Au 4f spectrum exhibited two peaks due to spin-orbit splitting doublets at 87.81 eV and 84.14 eV, corresponding to $4f_{5/2}$ and $4f_{7/2}$ metallic Au. Similarly, the high-resolution S 2p spectrum shows two peaks due to spin-orbit coupling at 169.99 eV and 168.81 eV corresponding to S $2p_{1/2}$ and S $2p_{3/2}$, respectively, which is assigned to sulfite and Na 1s with a singlet around 1071.65 eV (Fig. S25).

## References


1 T. K. Sau and C. J. Murphy, *J. Am. Chem. Soc.*, 2004, **126**, 8648–8649.
2 A. Miranda, E. Malheiro, E. Skiba, P. Quaresma, P. A. Carvalho, P. Eaton, B. de Castro, J. A. Shelnutt and E. Pereira, *Nanoscale*, 2010, **2**, 2209–2216.
3 Z. Guo, X. Fan, L. Liu, Z. Bian, C. Gu, Y. Zhang, N. Gu, D. Yang and J. Zhang, *J. Colloid Interface Sci.*, 2010, **348**, 29–36.
4 B. D. Busbee, S. O. Obare and C. J. Murphy, *Adv. Mater.*, 2003, **15**, 414–416.
5 S. S. R. Gupta, M. L. Kantam and B. M. Bhanage, *Nano-Struct. Nano-Objects*, 2018, **14**, 125–130.
6 J. E. Millstone, S. Park, K. L. Shuford, L. Qin, G. C. Schatz and C. A. Mirkin, *J. Am. Chem. Soc.*, 2005, **127**, 5312–5313.
7 J. Wang, L. Wang, J. Di and Y. Tu, *Sensors and Actuators B: Chemical*, 2008, **135**, 283–288.
8 G. Stremsdoerfer, H. Perrot, J. R. Martin and P. Cléchet, *J. Electrochem. Soc.*, 1988, **135**, 2881.
9 H. Ohlin, T. Frisk, M. Åstrand and U. Vogt, *Micromachines*, 2022, **13**, 452.
10 A. M. Sullivan and P. A. Kohl, *J. Electrochem. Soc.*, 1995, **142**, 2250.
11 P. Wilkinson, *Gold Bull.*, 1986, **19**, 75–81.

12 T. A. Green, *Gold Bul.l*, 2007, **40**, 105–114.
13 A. Gemmier, W. Keller, H. Richter and K. Ruess, *Plat. Surf. Finish*, 1994, **81**, 52–58.
14 E. Smalbrugge, B. Jacobs, S. Falcone, E. J. Geluk and F. Karouta, *Proceedings of the 5th annual symposium of the IEEE/LEOS Benelux Chapter : October 30, 2000, Delft , the Netherlands*, 2000, 143–146.
15 H. Honma and K. Hagiwara, *J. Electrochem. Soc.*, 1995, **142**, 81.